



National Defence
Research and
Development Branch

Défense nationale
Bureau de recherche
et développement

TECHNICAL MEMORANDUM 96/209

September 1996

TIME SPREADING AT HIGH FREQUENCY
IN A
SHALLOW WATER CHANNEL

Paul C. Hines — Arthur J. Collier — J. Stuart Hutton

19961115 054

**Defence
Research
Establishment
Atlantic**



**Centre de
Recherches pour la
Défense
Atlantique**

Canada

DTIC QUALITY INSPECTED 3

DISTRIBUTION STATEMENT A

Approved for public release;
Distribution Unlimited

DEFENCE RESEARCH ESTABLISHMENT ATLANTIC

9 GROVE STREET

P.O. BOX 1012
DARTMOUTH, N.S.
B2Y 3Z7

TELEPHONE
(902) 426-3100

CENTRE DE RECHERCHES POUR LA DÉFENSE ATLANTIQUE

9 GROVE STREET

C.P. BOX 1012
DARTMOUTH, N.É.
B2Y 3Z7



National Defence
Research and
Development Branch

Défense nationale
Bureau de recherche
et développement

TIME SPREADING AT HIGH FREQUENCY IN A SHALLOW WATER CHANNEL

Paul C. Hines — Arthur J. Collier — J. Stuart Hutton

September 1996

Approved by C.W. Bright
Deputy Director General

Distribution Approved by C.W. Bright


Deputy Director General

DREA TECHNICAL MEMORANDUM 96/209

Defence
Research
Establishment
Atlantic



Centre de
Recherches pour la
Défense
Atlantique

Canada

ABSTRACT

Time spreading measurements provide an indirect measure of the acoustic bandwidth that can be supported by the water channel, which is critical to the design of sonar systems. Time spreading measurements were collected in a water channel 100 m deep, off the coast of Nova Scotia. Data were collected at frequencies of 20-22 kHz, 27-29 kHz, and 35-37 kHz using linear FM pulses 2 s in duration. The experiments were part of a collaborative TTCP trial known as Trial Scotian (HF) organized by the Environmental Acoustic specialists group of GTP-11, Underwater Weapons and Countermeasures. Canada, the US, and the UK participated in the trial. Canada's SEAHORSE array, an anchored, high frequency active sonar was employed for the source-receiver, and a UK free drifting echo repeater was employed for the target. Source-receiver and target position were recorded using a portable tracking range operated by the US. In the paper, time spreading measurements are compared with modelled estimates obtained using the Generic Sonar Model (GSM). The GSM estimates of time spreading due to multipath propagation compare favourably with the experimental data. However, time spreading of individual paths – beyond the model predictions – is also evident. Additionally, the data were used to compute the standard deviation of the received echo intensity at each frequency. The standard deviation was computed two different ways. First it was computed using the peak echo level from each of the pulses at a given frequency. Then, it was computed from the total energy received from each of the pings. At all three frequencies, the standard deviation was lower by 1 to 2 dB when computed from the total received energy.

RÉSUMÉ

Les mesures d'étalement dans le temps fournissent une mesure indirecte de la largeur de bande acoustique que peut accepter le canal de son dans l'eau, ce qui est une donnée critique pour la conception des systèmes sonar. Les mesures d'étalement dans le temps ont été recueillies dans un canal d'une profondeur de 100 m, au large de la côte de la Nouvelle-Écosse. Les données ont été recueillies aux fréquences 20 - 22 kHz, 27 - 29 kHz et 35 - 37 kHz, en utilisant des impulsions FM linéaires d'une durée de 2 s. Les expériences faisaient partie d'un essai de collaboration du programme de coopération technique TTCP, appelé Trial Scotian (HF) (essai HF de la Nouvelle-Écosse), organisé par le groupe de spécialistes de l'acoustique environnementale du programme technique GTP-11, contre-mesures et armes sous-marines. Le Canada, les États-Unis et le Royaume-Uni ont participé à cet essai. Le réseau canadien SEAHORSE, sonar actif haute fréquence ancré, servait de source et de récepteur, tandis qu'un répéteur d'écho à dérive libre servait de cible. Les positions de la source et du récepteur, d'une part, et celles de la cible, d'autre part, ont été enregistrées à l'aide d'une installation de poursuite exploitée par les É.-U. La communication compare les mesures d'étalement aux estimations obtenues au moyen du logiciel Generic Sonar Model – GSM (modèle de sonar générique) à partir des données géométriques de l'expérience. Les estimations GSM de l'étalement dans le temps dû à la propagation sur divers trajets se compare favorablement aux données expérimentales. Toutefois, pour des trajets individuels, on constate aussi un étalement dans le temps dépassant celui qui était prévu par le GSM. De plus, les données ont servi à calculer l'écart type de l'intensité de l'écho reçu à chaque fréquence. L'écart type a été calculé de deux manières différentes, d'abord à partir du niveau d'écho de crête de chaque impulsion à une fréquence donnée, puis à partir de l'énergie totale reçue de chaque impulsion sonar. Aux trois fréquences, l'écart type calculé à partir de l'énergie totale reçue était inférieur de 1 à 2 dB au résultat obtenu par l'autre méthode.

DREA TM 96/209

**TIME SPREADING AT HIGH FREQUENCY IN A SHALLOW
WATER CHANNEL**

by

Paul C. Hines, Arthur J. Collier, J. Stuart Hutton

Defence Research Establishment Atlantic, P.O. Box 1012, Dartmouth, Nova Scotia,
Canada, B2Y 3Z7

EXECUTIVE SUMMARY

Background

It is well known that increasing the frequency bandwidth of a sonar pulse can increase the spatial resolution, and therefore improve target localization. One might mistakenly argue then, that increasing the sonar's bandwidth will always enhance its performance. However, the response of the water channel to the sonar signal places an upper limit on the improvement that one may achieve. In effect, the water channel itself is bandwidth limited.

Time spreading measurements provide an indirect measure of the acoustic bandwidth that can be supported by the water channel, which is critical to the design of a sonar system. The sonar designer uses this information to optimize the transmit pulse employed in the sonar. Decisions such as the pulse length, the pulse type, and the frequency bandwidth are all based in part on the time spreading characteristics of the water channel.

Results

Time spreading measurements were collected in a water channel 100 m deep, off the coast of Nova Scotia. Data were collected at frequencies of 20-22 kHz, 27-29 kHz, and 35-37 kHz using linear FM pulses 2 s in duration. The experiments were part of a collaborative TTCP trial known as Trial Scotian (HF) organized by the Environmental Acoustic specialists group of GTP-11, Underwater Weapons and Countermeasures. Canada, the US, and the UK participated in the trial. The trial's location reflects the increased interest in littoral waters expressed by the Canadian Navy.

In the paper, time spreading measurements are compared with modelled estimates obtained using the Generic Sonar Model (GSM). The GSM estimates of time spreading due to multipath propagation compare favourably with the experimental data. However, time spreading of individual paths – beyond the model predictions – is also evident. The results of this study will be used to improve performance predictions of present day sonars as well as to aid in the design of future sonars.

TABLE OF CONTENTS

ABSTRACT	ii
RÉSUMÉ	ii
EXECUTIVE SUMMARY	iii
Background	iii
Results	iii
TABLE OF CONTENTS	iv
INTRODUCTION	1
I. EXPERIMENTAL EQUIPMENT AND GEOMETRY	1
A. The SEAHORSE System	1
B. The DEMONSTRATOR Echo Repeater	4
II. ENVIRONMENTAL DESCRIPTION	4
A. Benthic Topography	4
B. The Water Column	4
III. THE TIME SPREADING EXPERIMENT	7
A. Time Spreading at 21 kHz.....	7
B. Time Spreading at 28 kHz	9
C. Time Spreading at 36 kHz	12
IV. COMPARISON OF TIME SPREADING DATA TO GSM	12
A. GSM/Data Time Spreading Comparisons at 21 kHz	16
B. GSM/Data Time Spreading Comparisons at 28 kHz	16
C. GSM/Data Time Spreading Comparisons at 36 kHz	17
V. DISCUSSION	17
VI. SUMMARY AND CONCLUSIONS	19
ACKNOWLEDGMENTS	20
REFERENCES	20

INTRODUCTION

This paper presents measurements of time spreading over the frequency band 20 kHz - 40 kHz, collected in a shallow water channel off the coast of Nova Scotia. Time spreading measurements provide an indirect measure of the (water) channel bandwidth which is critical to the design of sonar systems. The measurements are compared with predictions obtained using the Generic Sonar Model¹ (GSM).

The experimental measurements were part of a collaborative TTCP trial known as Trial Scotian (HF) organized by the Environmental Acoustic specialists group of GTP-11, Underwater Weapons and Countermeasures. Canada, the US, and the UK participated in the trial. Additional measurements made during the trial from DREA's high-frequency SEAHORSE array² included submarine target strength, surface ship target strength, high frequency ambient noise, shallow water reverberation, and frequency spreading. The results from these experiments as well as (water) channel characterization measurements made with a US General Test Vehicle (GTV) will be reported separately.

Following the introduction we describe the experiment and the bottom topography of the experimental site. Then the time spreading data are presented and compared with estimates obtained using GSM. Finally, we present some conclusions which resulted from the research.

I. EXPERIMENTAL EQUIPMENT AND GEOMETRY

Figure 1 shows a schematic of the geometry for the time spreading experiment. The UK echo repeater was deployed to 76 m depth; SEAHORSE was deployed to 42 m. The seabed was nominally flat, with an average water depth over the extent of the experiment of 104 m. The benthic topography is discussed in greater detail in the following section. The experiment was conducted inside the perimeter of a portable tracking range developed and operated by personnel from Naval Undersea Warfare Center (NUWC), Division Keyport. SEAHORSE was decoupled from surface motion using its two-stage decoupling system² and anchored to the seabed within the tracking range using a second two-stage decoupling system. The experiment was conducted during a 2 hour period throughout which the echo repeater was free drifting. This allowed for time spreading measurements at several SEAHORSE-to-target ranges. Figure 2 shows a plot of the SEAHORSE and the echo repeater GPS tracks measured during the experiment. The start locations of the tracks are as marked. Figure 3 contains a plot of relative range and bearing from SEAHORSE to the echo repeater over the duration of the experiment. The data in Figure 3 equate to an average drift speed for the echo repeater of 0.1 m/s.

A. The SEAHORSE System

SEAHORSE is a HF active sonar for collecting environmental acoustic data in the open ocean. The sonar operates over the frequency band 20 kHz to 40 kHz and has an approximately symmetrical beamwidth of 0.1 steradians. In conjunction with the acoustic sensors, SEAHORSE is instrumented with a range of non-acoustic sensors to assist in the evaluation of the data. The non-acoustic sensors include depth, tilt, roll, and heading sensors, to monitor array position and direction, as well as accelerometers to monitor platform motion. A series of motors contained in the sonar head – and remotely controlled from a research ship – point the sonar head to the required azimuth and tilt.

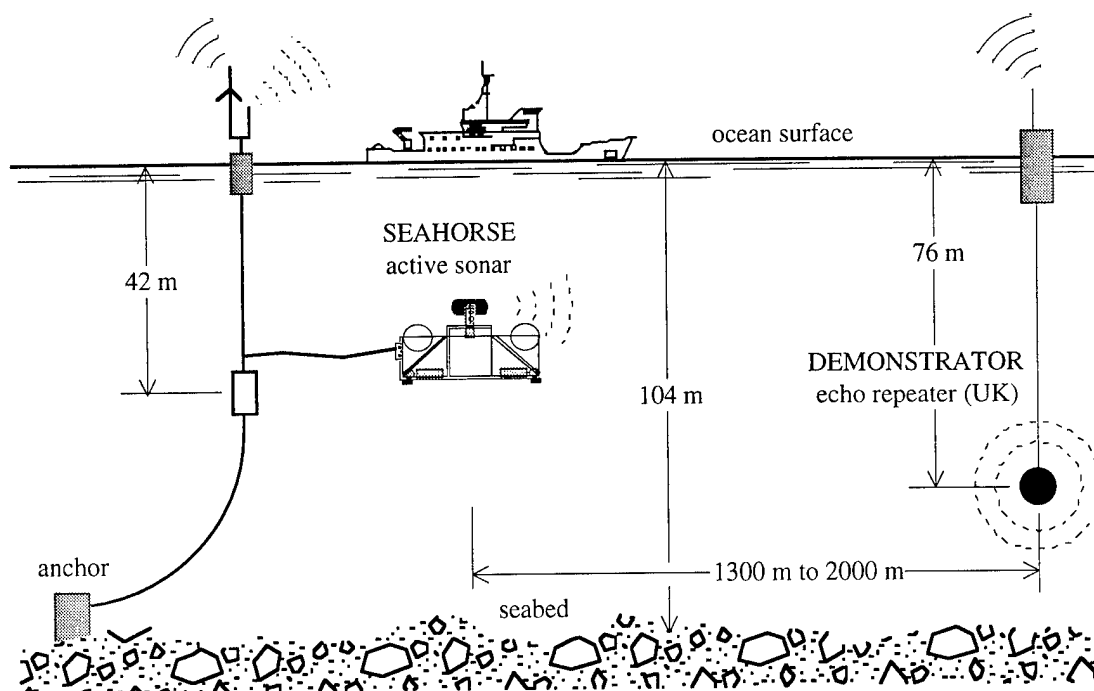


Figure 1: Schematic of experimental setup. Note that the echo-repeater was free drifting during the experiment thereby varying the range from 1300 m to 2000 m.

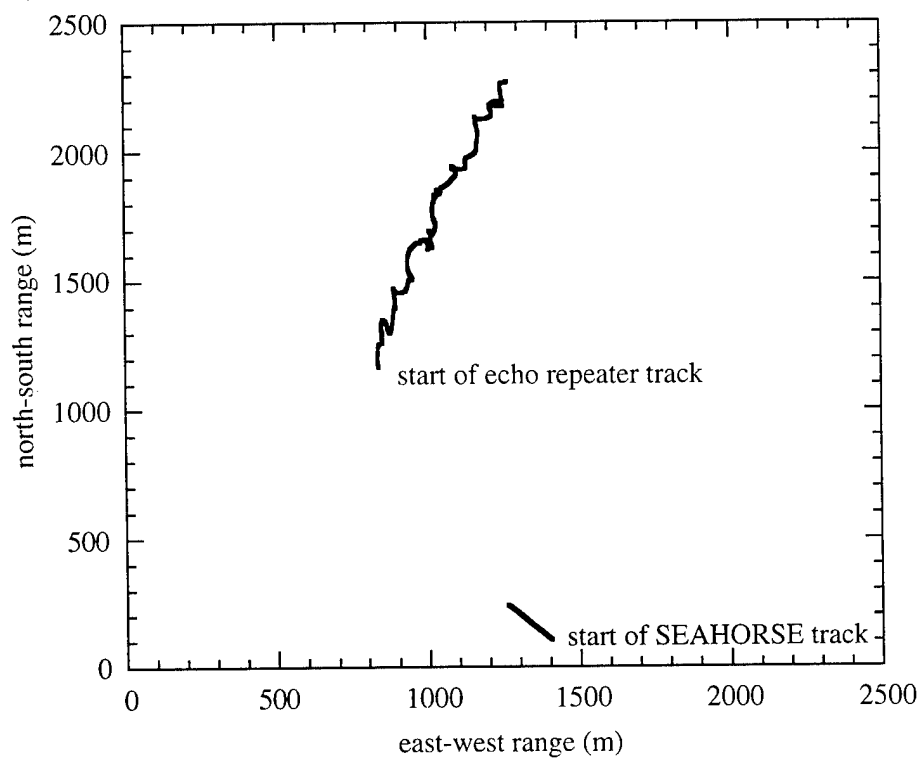


Figure 2: Tracks of SEAHORSE and echo repeater during the experiment.

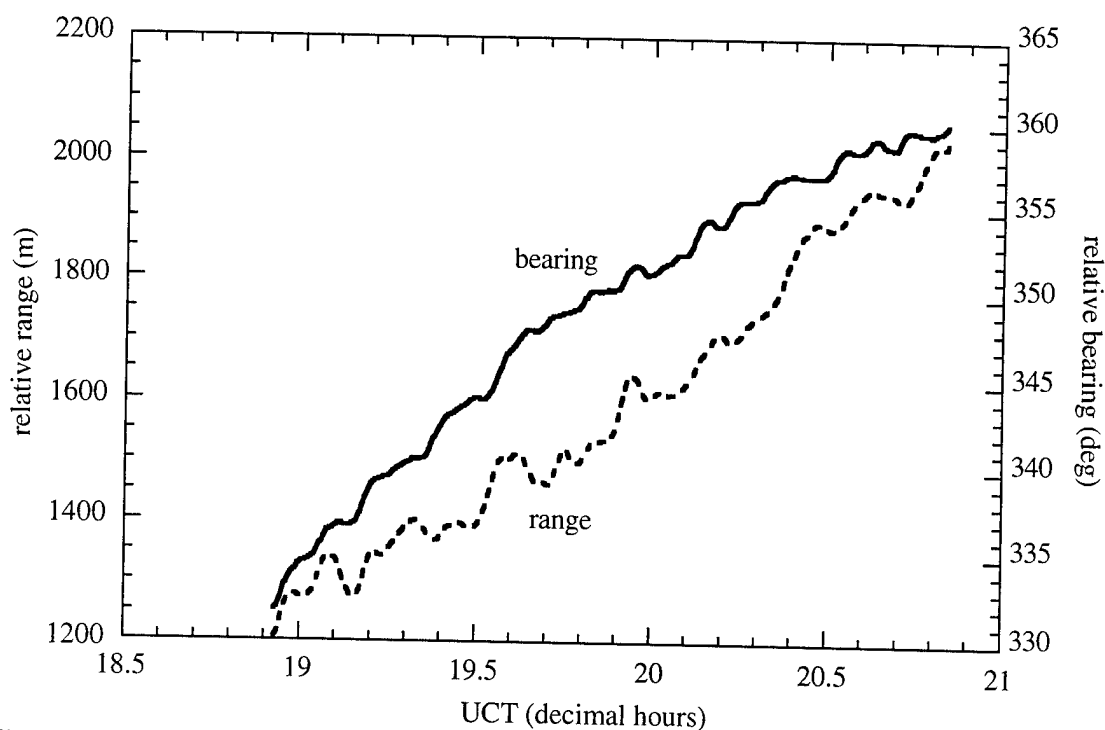


Figure 3: Relative range and bearing from SEAHORSE to the echo repeater during the experiment.

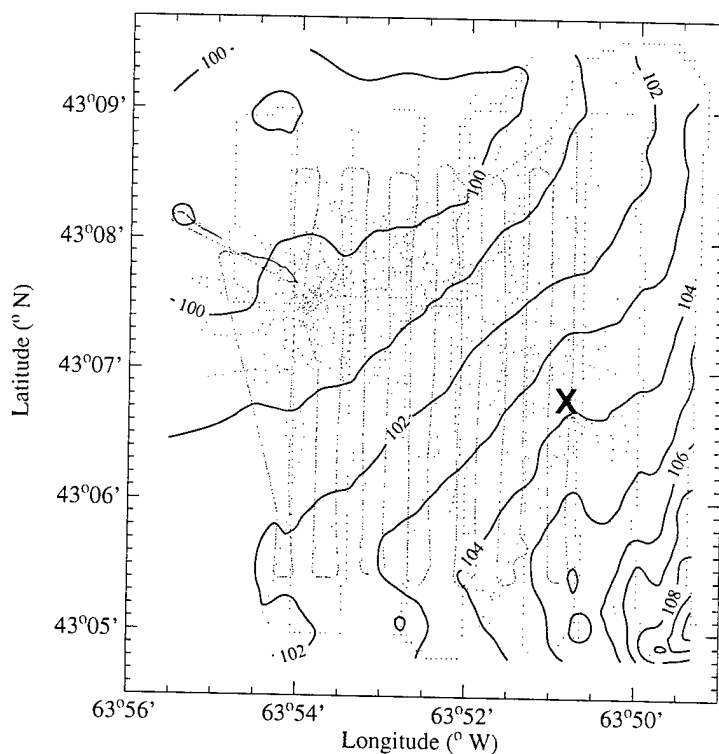


Figure 4: Contour plot of the water depth (in meters) at the experimental site. The dots mark the location of echosounder readings from which the contours were extrapolated. The location of SEAHORSE during the experiment is denoted by an X.

Communication between the research ship and SEAHORSE is handled via two RF links. The first is a one-way UHF data link operating at 2.37 GHz which is used to transmit the acoustic and non-acoustic data collected by SEAHORSE back to the ship. The second is a two-way VHF command link operating at 462 MHz which is used to maintain system control (e.g. select pulse type, set amplifier gains, control pointing direction, etc.).

The transmitter consists of a 48-element array of transducers, shaded such that one obtains an approximately conical beam of 0.1 steradians, measured to the -3 dB points. (In cross-section, this equates to a two-sided beamwidth of 20°.) Beam steering is accomplished through purely mechanical means. The sonar operates across the frequency band 20 kHz to 40 kHz with a source strength of 202 ± 3 dB re $1 \mu\text{Pa}$ @ 1m. The same 48-element array used for the acoustic transmitter is used as the primary acoustic receiver. As a receiver, the 48-element array of transducers is shaded to obtain an approximately conical beam of 0.1 steradians, measured to the -3 dB points. The receive sensitivity is -180 ± 5 dB re $1 \mu\text{Pa}/\text{Hz}$ across the frequency band 20 to 40 kHz.

B. The DEMONSTRATOR Echo Repeater

DEMONSTRATOR is a free-drifting echo repeater designed and operated by the UK's Defence Research Agency (DRA). System control is maintained through a VHF command link operating at (nominally) 400 MHz. DEMONSTRATOR can be programmed to operate at center frequencies of 22, 28, or 37 kHz with a bandwidth at any of these center frequencies of 4 kHz. The target strength is also programmable and was set to +10 dB during the entire experiment. Both the transmitter and the receive hydrophone are omnidirectional. As well as returning a duplicate of the received signal, DEMONSTRATOR returns a 19 m/s Doppler shifted version of the signal following a delay of 200 ms. The system contains an onboard DAT recorder with a tape storage capacity of two hours. The system has a battery life of 4 to 6 hours continuous, but can be shut down and reactivated as desired to extend system life.

II. ENVIRONMENTAL DESCRIPTION

A. Benthic Topography

The site of the experiment was the eastern flank of the La Have Bank, about 100 nautical miles south of Halifax, Nova Scotia. Figure 4 contains a contour plot of the bottom for the experimental site. The dots overlaid on the plot mark locations of bottom depth measurements taken using the bathymetric system on CFAV QUEST, the research ship employed for the sea trial. The contour lines were constructed from these depth measurements. The location of SEAHORSE is denoted in the figure by an X. The bathymetric measurements were also used to generate the surface plot of the benthic interface presented in Figure 5. These plots show that the bottom had a gentle slope to the southeast, with the depth increasing from 100 to 110 m over about 10 km. Although there is little small-scale variability in the bathymetry, the bottom at the site is rough. Side scan sonar and visual records collected at the site during a subsequent trial showed the bottom at the site to be rough to very rough. The bottom is predominately cobble, with the smoothest areas consisting of coarse gravel. In the roughest areas, cobbles were the order of 0.3 to 3.0 m diameter.

B. The Water Column

Figure 6 shows the sound-speed profile for the site taken shortly after the experiment. The minimum speed occurred at 42 m depth, coinciding (approximately)

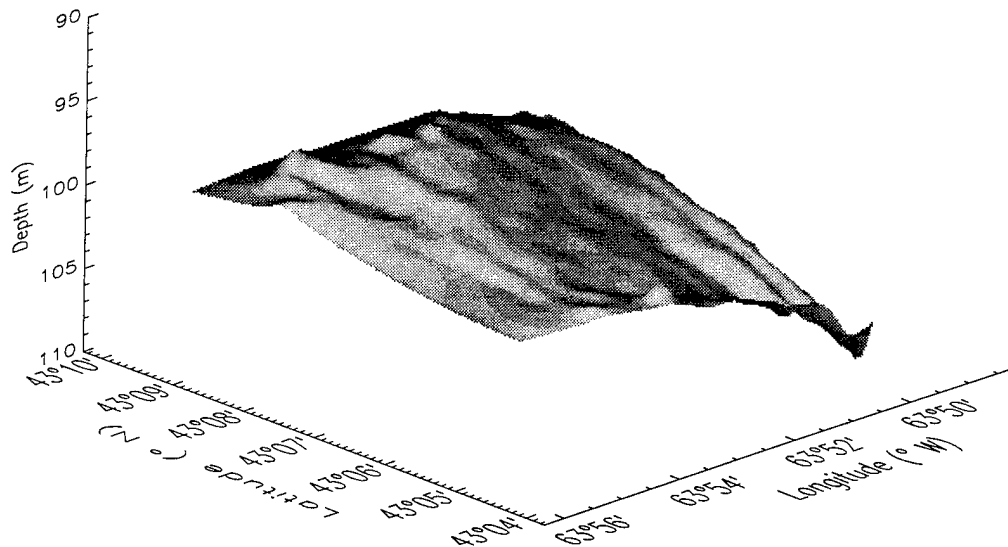


Figure 5: Surface plot of the seabed at the experimental site. The figure was constructed from the echosounder readings shown in Figure 4.

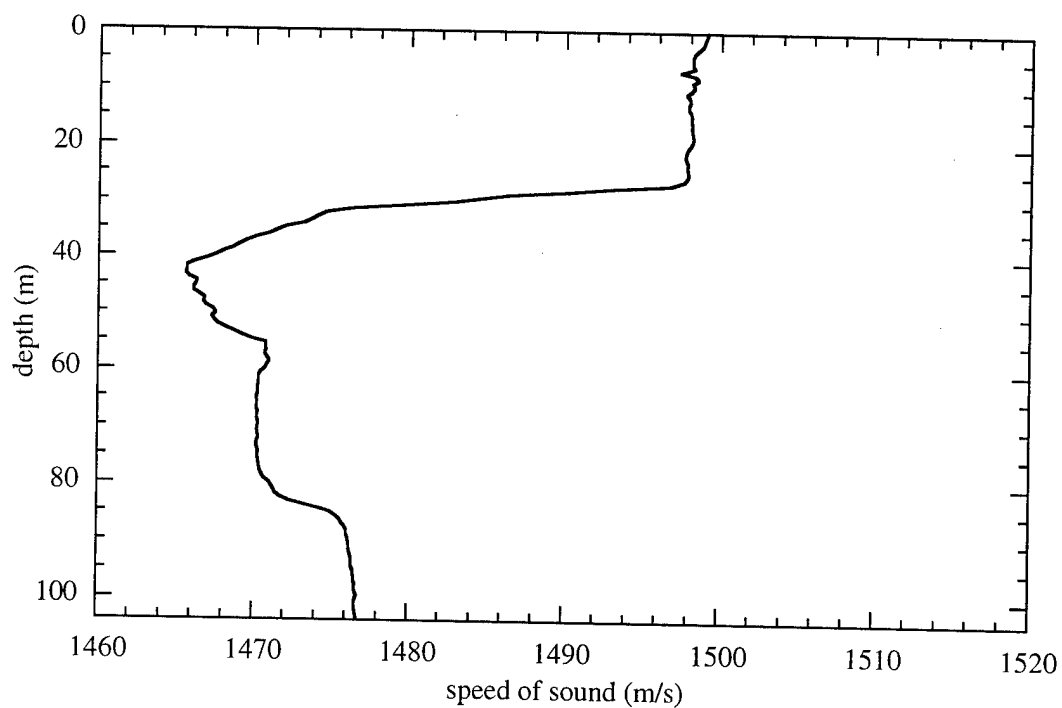


Figure 6: Sound-speed profile of the water column taken shortly after the experiment.

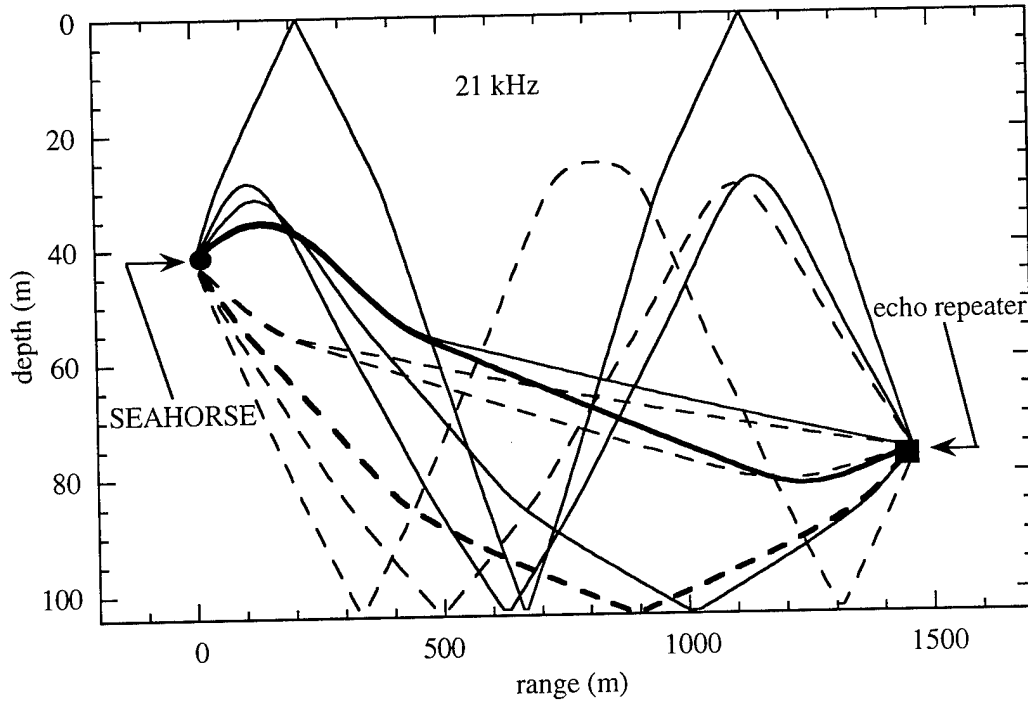


Figure 7: The 10 dominant eigenrays between the SEAHORSE transmitter and the echo repeater for the 21 kHz geometry. For clarity, rays departing the source toward the surface are solid lines and rays departing the source toward the bottom are dashed. The bold solid line is the most intense ray and the bold dashed line is the first arrival.

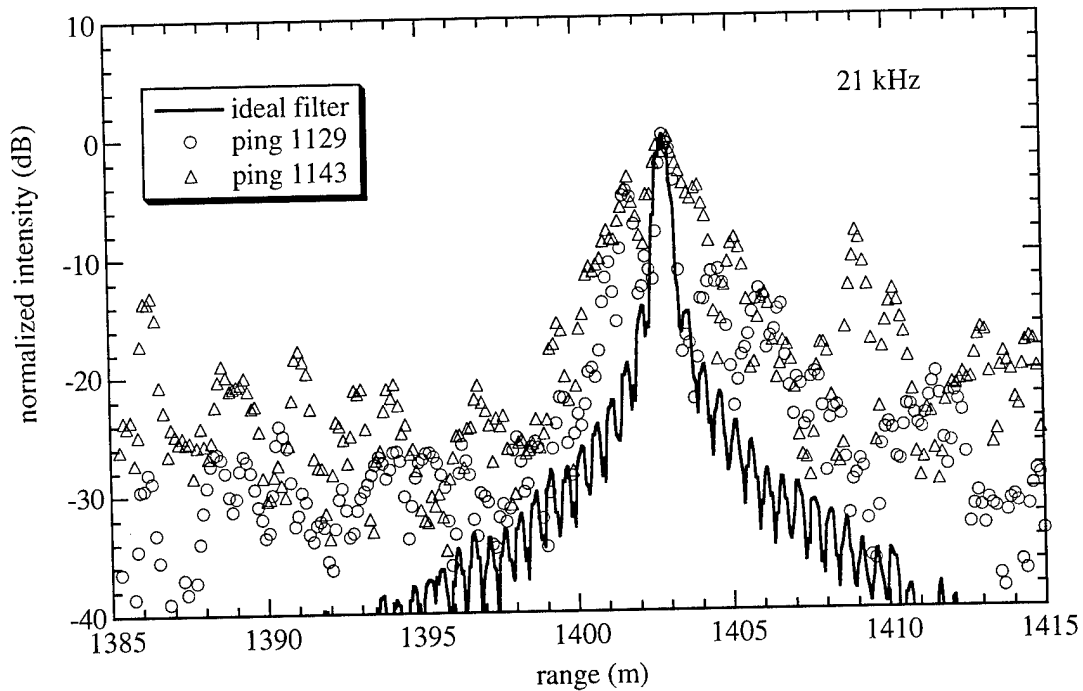


Figure 8: Target returns from the echo repeater for two "typical" linear FM pings compared to the idealized output of the matched filter (solid line) illustrating time spreading in the received echoes.

with the SEAHORSE depth. Figure 7 contains the eigenrays from SEAHORSE to the echo repeater for the 10 most intense rays, for a source frequency of 21 kHz. In this and subsequent figures, a nominal sound speed of 1470 m/s was used to convert time units to range. As one can see from the ray paths, the sound-speed profile of Figure 6 resulted in limited surface bounce paths from SEAHORSE to the echo repeater for our experimental geometry.

III. THE TIME SPREADING EXPERIMENT

The time spreading experiment ran for approximately 2 hours. The entire experiment was conducted in sea state 5 and the wind was reasonably steady at 12 to 15 m/s (24 to 30 knots). Four pulse types were used during the experiment. The results of three of them, the linear FM pulses (LFM) are included in this report. Results using the fourth pulse type, a stepped CW, are reported elsewhere³. Each of the 3 LFM pulses were 160 ms duration with 25% Tukey shading (12.5% at the start of the pulse and 12.5% at the end of the pulse). The three LFM's had 2-kHz bandwidths spanning frequencies of 20-22 kHz, 27-29 kHz, and 35-37 kHz, respectively. This equates to a temporal resolution (to the -3 dB points) of approximately ± 0.17 ms; or assuming an acoustic wave speed of 1470 m/s, a range resolution of ± 0.25 m. Throughout the remainder of this paper, each pulse type is referred to by its center frequency: 21, 28, or 36 kHz.

At each frequency, a sequence of 25 LFM pulses was transmitted with a repetition rate from pulse-to-pulse of 15 seconds. For each transmitted pulse, data were recorded for approximately 4 seconds, starting about 240 ms prior to transmit. We calculated the range from SEAHORSE to the echo repeater acoustically by using the time delay between the start of the transmit pulse and reception of the echo repeater return. Sync dropouts in the data telemetry link – due to high seas – resulted in a loss of 5-9 LFM pulses in each sequence. Analysis was performed on sixteen pulses from each sequence so that the number of time series examined was consistent at all frequencies. During analysis the pulses were heterodyned down in frequency to the band 500 - 2500 Hz, low-pass filtered, and sub-sampled by a factor of 8 to reduce data processing and storage requirements. The time series recorded for each pulse was segmented into 4-kiloword samples (50% overlap between samples) and Fourier transformed. The data were matched filtered in the frequency domain using fast convolution. The resulting time spreading data were converted to an equivalent range by assuming a sound speed of 1470 m/s. It may appear somewhat odd to convert *time* spreading data to *range* units. However, it is primarily the effect that time spreading has on range resolution that makes time spreading such an important issue.

A. Time Spreading at 21 kHz

Figure 8 contains a plot of the time spreading returns from two LFM pulses for the 21 kHz run. Each return is normalized to 0 dB at its respective maximum. The two curves were time shifted to align the peak return from the echo repeater for each ping.⁴ The range from SEAHORSE to the echo repeater, based on the dominant arrival, was approximately 1400 m. The open circles and triangles represent the data. The solid line shown in the figure represents the spatial resolution of the matched filter using an exact duplicate of the kernel as the input signal, that is to say, the idealized output of the matched filter. The echo returns typify the ping-to-ping variability in the time spreading data of all 16 of the 21-kHz LFM pulses that were collected. From the figure, one can see that the data are time spread significantly below the -4 dB level.

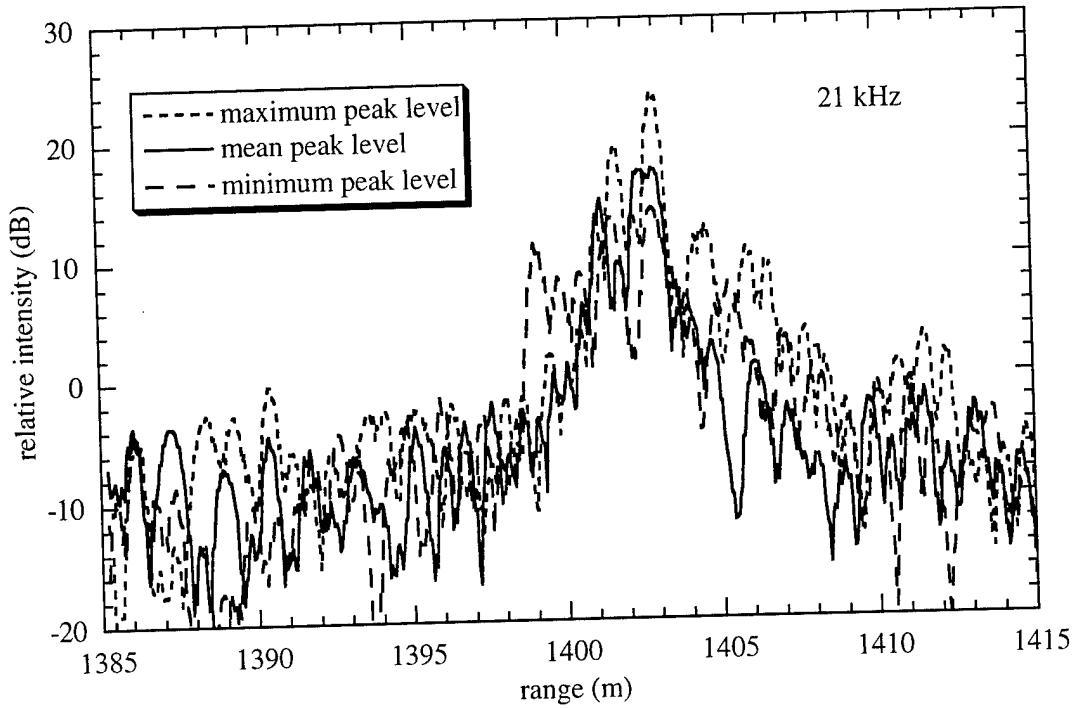


Figure 9: Time spreading data for the maximum, mean (see footnote 5), and minimum target returns, measured relative to the dominant eigenray path, for each of the 16 pulses at 21 kHz.

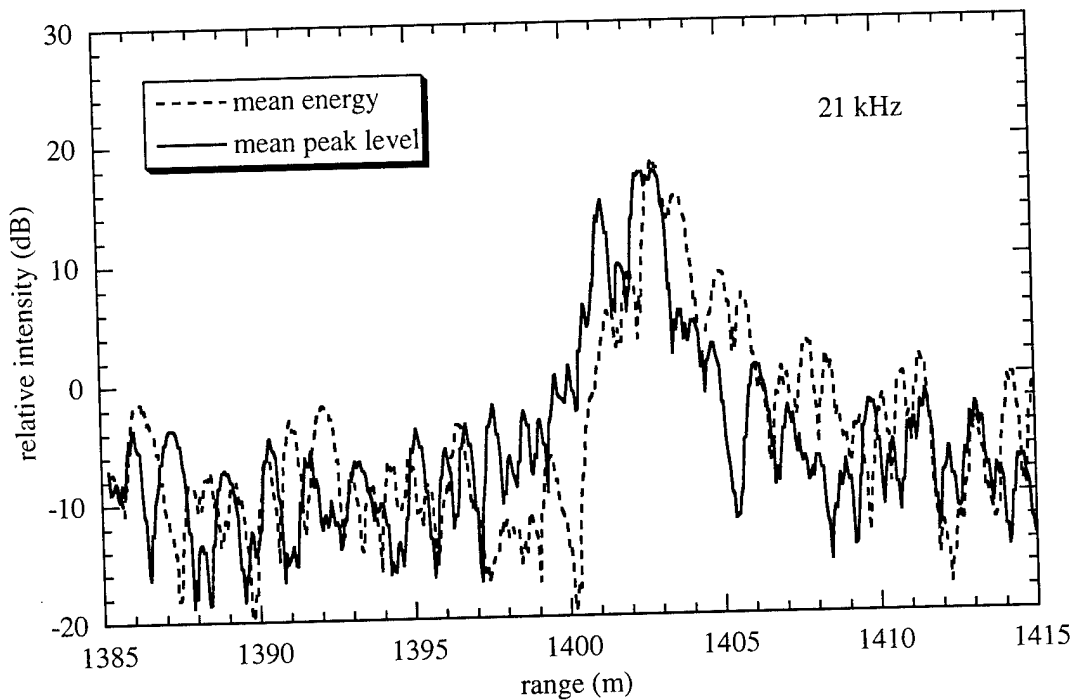


Figure 10: Time spreading data for the mean target return (see footnote 5), measured relative to the total energy returned by the target via all paths, for each of the 16 pulses at 21 kHz. For comparison the mean level measured relative to the dominant eigenray path is replotted from Figure 9.

To indicate the variability in the received echoes, Figure 9 shows a plot of the time spreading data for target returns from three of the 21 kHz LFM pulses. The data plotted are the echo levels for the maximum, the minimum, and the mean⁵ target returns as measured relative to the dominant eigenray path (i.e. the peak level of the curve), for the 21 kHz pulses. Using the peak level from each of the 21 kHz LFM pulses, one obtains a standard deviation⁶ of 2.3 dB. Alternatively, one may describe the strength of an echo in terms of the *total energy*⁷ returned by the target via all paths. Using this definition one obtains a standard deviation of 1.7 dB for the 16 pulses at 21 kHz. Figure 10 contains a plot of the data for the mean target return as measured relative to the total energy. For comparison the mean level measured relative to the dominant eigenray path is replotted from Figure 9. Table I lists the standard deviation using both approaches for the 21, 28, and 36 kHz data sets.

TABLE I. Standard deviation (σ) of the target echo for linear FM (LFM) pulses in individual frequency bands. The standard deviations are computed for echo strength expressed as peak amplitude and total received energy.

Frequency (kHz)	σ (dB) using peak level	σ (dB) using total energy
21	2.3	1.7
28	6.5	4.7
36	4.5	2.2

Figure 11 contains a plot of the average of the time spreading data, normalized to zero dB at its maximum, for the 21 kHz run. Prior to averaging, the matched-filtered data were time shifted to align the peak return from the echo repeater for each ping. The open circles represent the average of all 16 pings. The solid line in the figure shows the spatial resolution of the matched filter. This curve was generated by using an exact duplicate of the kernel as the input signal. To remain consistent with the data, the solid line was obtained by averaging the matched-filter output of 16 realizations of the input signal, each input signal having a slightly different time delay. In this way, any smearing of the data resulting from misalignment of the FFT window⁸ and the received echoes will be included in the ideal matched-filter curve. The averaged data substantiates the observation made earlier in reference to the individual pings show in Figure 8. That is: little or no time spreading occurs in the region of the peak, down to about -4 dB but below -4 dB the time spreading increases substantially. Furthermore, the averaged data indicates that the spreading is asymmetric about the maximum.

B. Time Spreading at 28 kHz

Figure 12 contains a plot of the time spreading data for target returns from three of the 28 kHz LFM pulses. The range from SEAHORSE to the echo repeater was approximately 1860 m. The data plotted in the figure are the matched-filter outputs for the maximum, the minimum, and the mean echoes, as measured relative to the dominant eigenray path, for the 28 kHz pulses. (Recall footnotes 4 and 5.) It is obvious from comparing Figure 12 to Figure 9 that there is greater variability in the received echoes at 28 kHz, than at 21 kHz. In more quantitative terms, one obtains a standard deviation of 6.5 dB from the peak levels from the sixteen 28 kHz pulses compared to 2.3 dB at 21 kHz. Using the total energy returned by the target via all paths, one obtains a standard deviation of 4.7 dB for the 16 pulses at 28 kHz. Figure 13 contains a plot of the 28 kHz data for the mean target return as measured relative to the total energy. (The curve representing the mean level measured relative to the dominant eigenray path is not reproduced from Figure 12 because at 28 kHz it happens to be the same ping.)

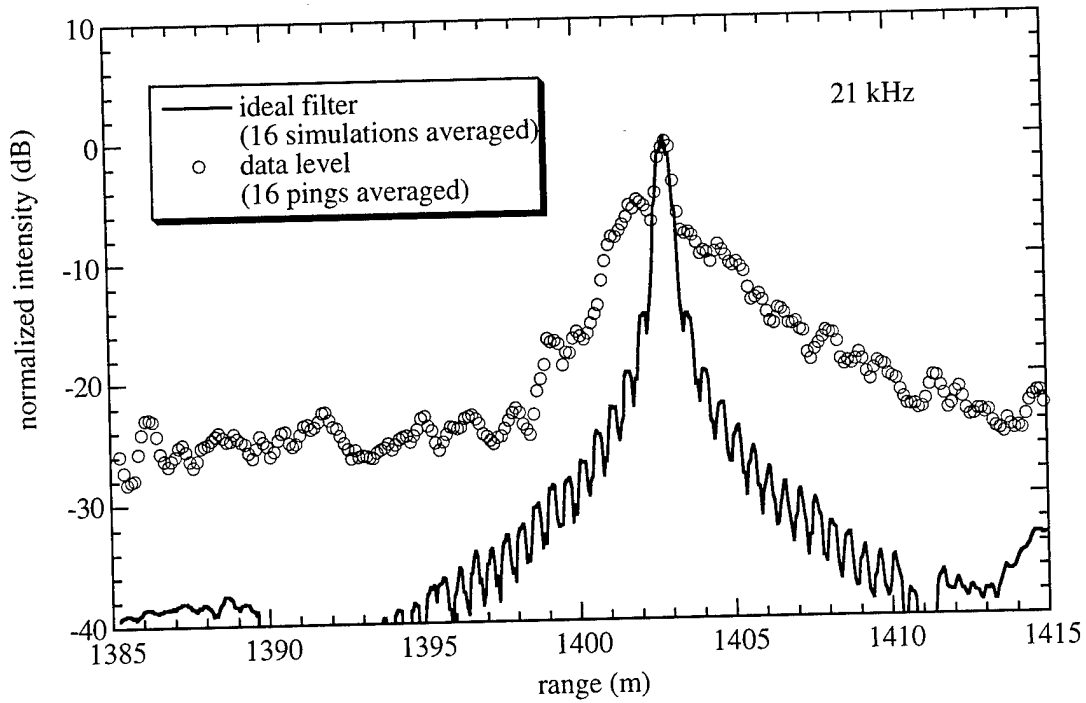


Figure 11: Averaged time spreading data for 16 pings (circles), normalized to 0 dB at its maximum, compared to the idealized output of the matched filter (solid line), for the 21 kHz run.

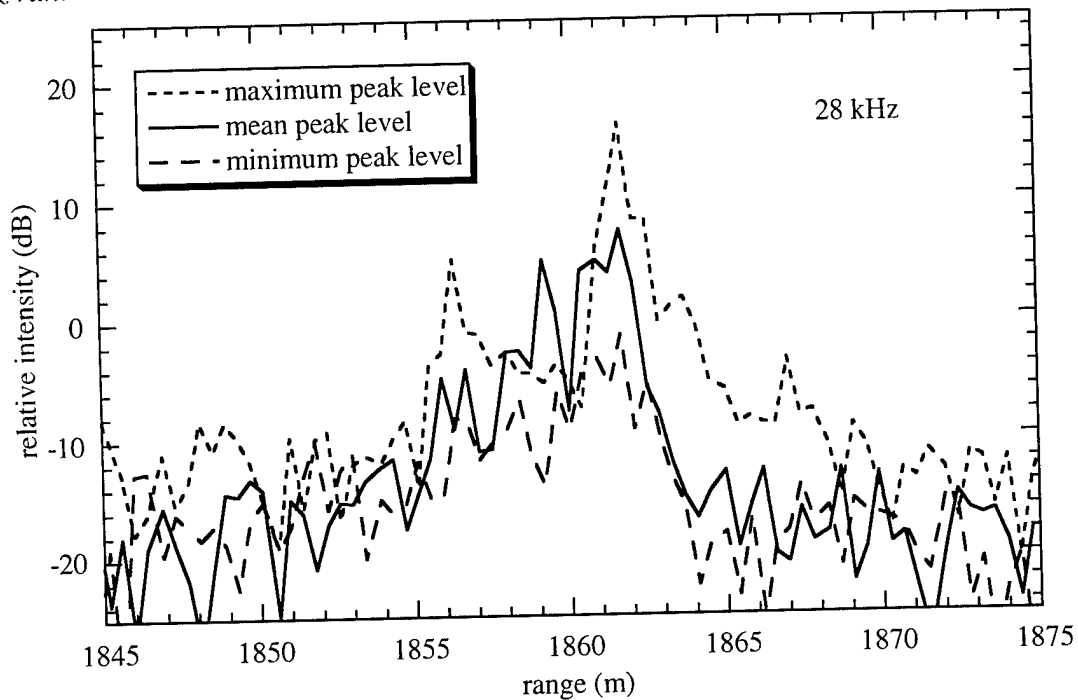


Figure 12: Time spreading data for the maximum, mean (see footnote 5), and minimum target returns, measured relative to the dominant eigenray path, for each of the 16 pulses at 28 kHz.

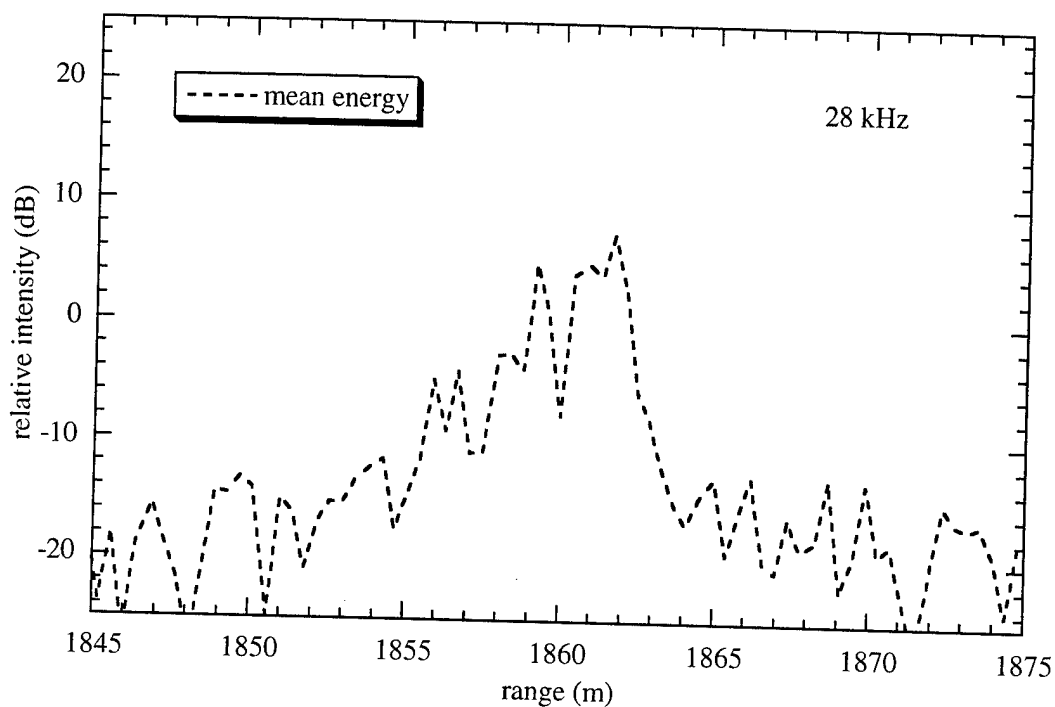


Figure 13: Time spreading data for the mean target return (see footnote 5), measured relative to the total energy returned by the target via all paths, for each of the 16 pulses at 28 kHz.

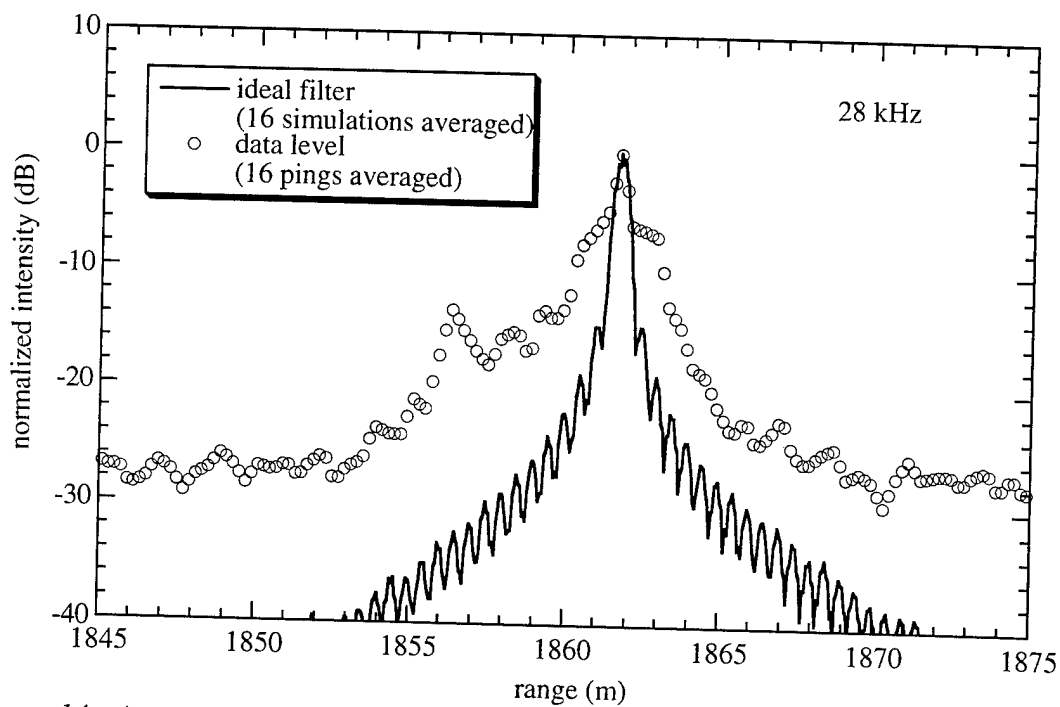


Figure 14: Averaged time spreading data for 16 pings (open circles), normalized to 0 dB at its maximum, compared to the idealized output of the matched filter (solid line), for the 28 kHz run.

Figure 14 contains a plot of the averaged time spreading data, normalized to 0 dB at its maximum, for the 28 kHz run. The solid line in the figure is the output of the idealized matched-filter, computed as described previously for Figure 11. Prior to averaging, the matched-filtered data were time shifted to align the peak return from the echo repeater for each ping. The open circles represent the average of all 16 pings. As was the case for 21 kHz, the 28 kHz data are time spread significantly below about the -4 dB level. However, in contrast to the 21 kHz case, the 28 kHz data are not as asymmetric about the maximum and the most significant time spreading occurs before, not after, the dominant eigenray arrival.

C. Time Spreading at 36 kHz

Figure 15 illustrates the variability of the time spreading measured at 36 kHz. The figure contains the matched-filter outputs (with peaks aligned) for the maximum, minimum and mean target returns as measured relative to the dominant eigenray path for three of the 36 kHz LFM pulses. The range from SEAHORSE to the echo repeater was approximately 1950 m. Using the peak level from each of the 36 kHz LFM pulses, one obtains a standard deviation of 4.5 dB. Using the total energy returned by the target via all paths, one obtains a standard deviation of 2.2 dB for the sixteen 36 kHz pulses. Figure 16 contains a plot of the 36 kHz data for the mean target return as measured relative to the total energy. For comparison the mean level measured relative to the dominant eigenray path is replotted from Figure 15.

Figure 17 contains a plot of the averaged time spreading data, normalized to zero dB at its maximum, for the 36 kHz run. The solid line in the figure is the output of the idealized matched-filter, computed as described previously for Figure 11. Prior to averaging, the matched-filtered data were time shifted to align the peak return from the echo repeater for each ping. The open circles represent the average of all 16 pings. The data in Figure 17 indicate that at 36 kHz, the time spread is only significant below the -8 dB level.

In the following section we compare the averaged time spreading data with results modelled using the Generic Sonar Model (GSM) to gain some insight into the cause of the measured time spreading.

IV. COMPARISON OF TIME SPREADING DATA TO GSM

Time spreading for the experimental geometry was modelled using GSM. Inputs to GSM included the transmit and receive beam patterns for SEAHORSE, the sound-speed profile of Figure 6, a wind speed of 27 knots, bottom reflection coefficients and bottom scattering strengths, and an omnidirectional target strength of 10 dB for the echo repeater. When running the model we assumed a pulse length of 0.67 ms to obtain a temporal resolution equivalent to that of the LFM pulses employed in the experiment.

The bottom backscattering strength was estimated using a Lambert's rule dependence with a coefficient of -27 dB, independent of frequency. Reverberation measurements made at the site support this backscatter dependence.⁹ The reverberation measurements also show that ambient noise, not reverberation provides the noise background for the echo-repeater returns at 28 kHz and 36 kHz. The bottom reflection coefficients proved the most difficult GSM inputs to estimate. This resulted from the lack of quantitative bottom information currently available for the site¹⁰. Table II contains the bottom loss coefficients employed. These numbers represent "reasonable"

values and provide an acceptable fit to the data. Note that the bottom reflection coefficient at grazing angles greater than 8° does not affect the results for this geometry.

TABLE II. *Bottom reflection coefficient table employed for GSM evaluation. Note that the bottom reflection coefficient at grazing angles greater than 8° does not affect the results for this geometry.*

Grazing angle (degrees)	Bottom reflection coefficient (dB)
0.0	-0.00
2.0	-2.00
4.0	-4.00
6.0	-6.00
8.0	-8.00
10.0	-8.00
20.0	-8.00
90.0	-8.00

The GSM predictions were obtained by calculating the dominant eigenrays (using MULTIP) from SEAHORSE to the target, (in this case the echo repeater) to obtain a series of arrivals at the target for a specific SEAHORSE-to-target range. The source level and arrival time of each of these eigenrays were then used as sources¹¹ at the echo repeater and propagated back to SEAHORSE. The signal excess subroutine CMPAX1 in GSM was modified in order to output the echo level plus reverberation level received at SEAHORSE. Finally, the eigenray arrival times were converted to range using a sound speed of 1470 m/s so as to remain consistent with the data. The ranges of the eigenray peaks can more appropriately be thought of as approximate path lengths for the various eigenrays (recall Figure 7).

As indicated in Figure 3 the echo repeater opened from SEAHORSE at a rate of approximately 0.1 m/s during the experiment. This drift rate resulted in a change of range of 30 to 80 m (1% to 3% of the total range) over the time taken to transmit the ping sequence at each frequency. The sensitivity of the modelled output to these range variations is indicated in Figure 18 in which the GSM results at 28 kHz for ranges of 1860 m, 1875 m, 1890 m, and 1905 m are shown. The four curves were time shifted to align the maximum of each curve. The ambient noise level lies at approximately -25 dB. Clearly, the amplitude and number of the peaks varies with even small changes in range. If the modelled returns are averaged, as was done with the experimental data, the peaks shown in the single modelled returns will be smeared. To include the range averaging effects in the modelled results, 16 GSM estimates were taken at each frequency to correspond to the 16 experimental pings. For simplicity, we calculated the start and stop range for each frequency sequence from the measured time delays and assumed a constant drift rate to estimate the intermediate ranges. The measured increase in range during both the 21 and 28 kHz experiments was 30 m and thus the model estimates were computed at 2 m range increments. The measured increase in range during the 36 kHz experiment was 75 m and thus the model estimates were computed every 5 m.

Recall from Table I that the standard deviation computed from the peak amplitudes of the 16 pings varied from 2.3 to 6.5 dB. These values are considerably greater than the standard deviation of the 16 model estimates, which was approximately 1 dB at all frequencies. That is to say, the ping-to-ping intensity fluctuations measured experimentally are largely unaccounted for in GSM. Therefore, when computing the average time spread from the data, each ping was normalized to zero dB at its maximum,

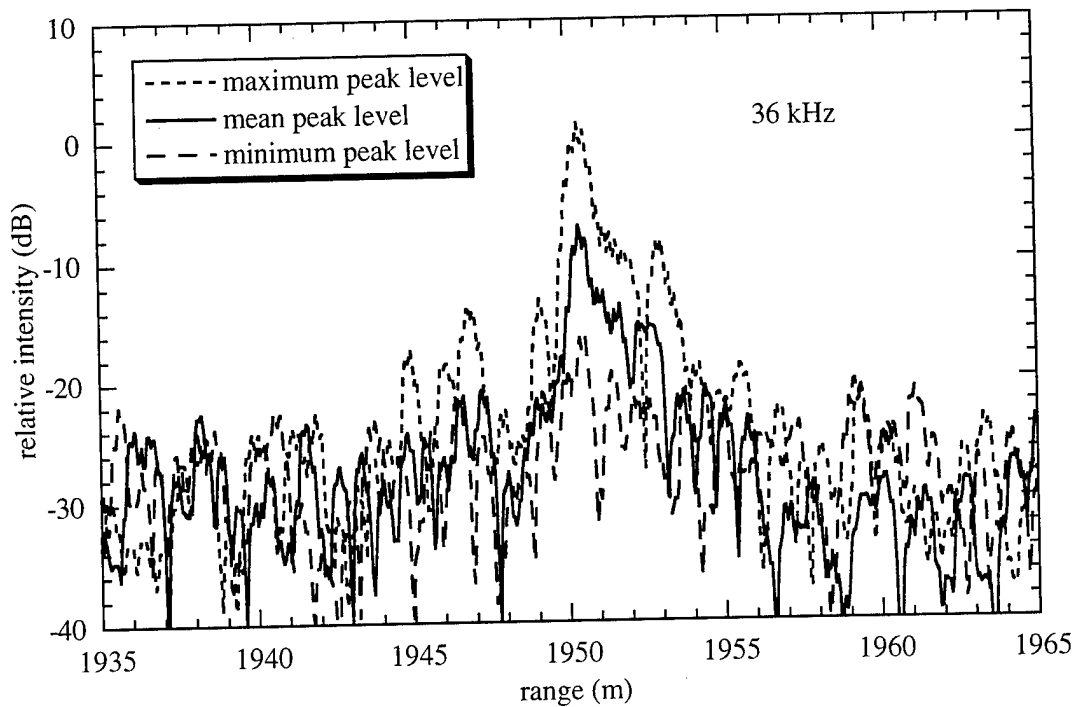


Figure 15: Time spreading data for the maximum, mean (see footnote 5), and minimum target returns, measured relative to the dominant eigenray path, for each of the 16 pulses at 36 kHz.

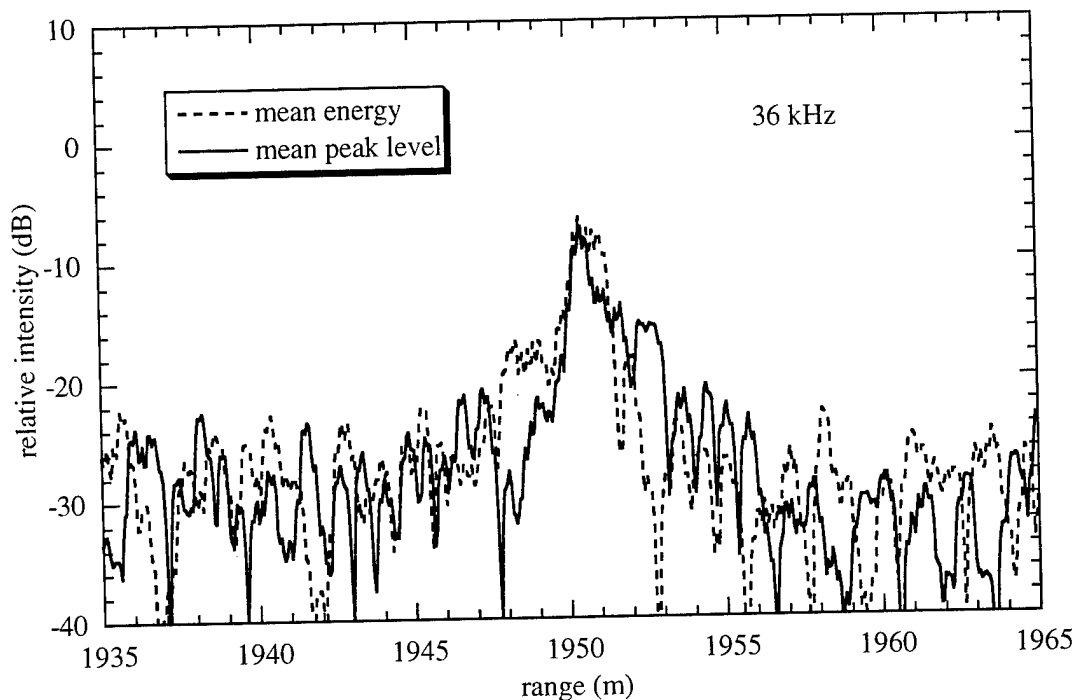


Figure 16: Time spreading data for the mean target return (see footnote 5), measured relative to the total energy returned by the target via all paths, for each of the 16 pulses at 36 kHz. For comparison the mean level measured relative to the dominant eigenray path is replotted from Figure 15.

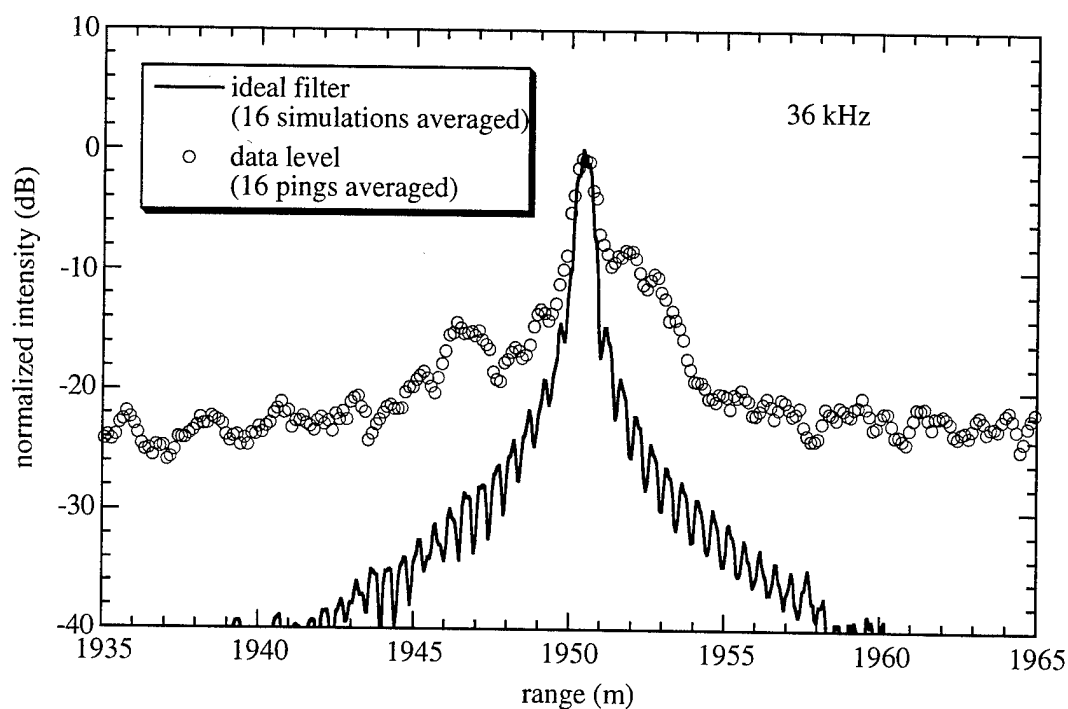


Figure 17: Averaged time spreading data for 16 pings (open circles), normalized to 0 dB at its maximum, compared to the idealized output of the matched filter (solid line), for the 36 kHz run.

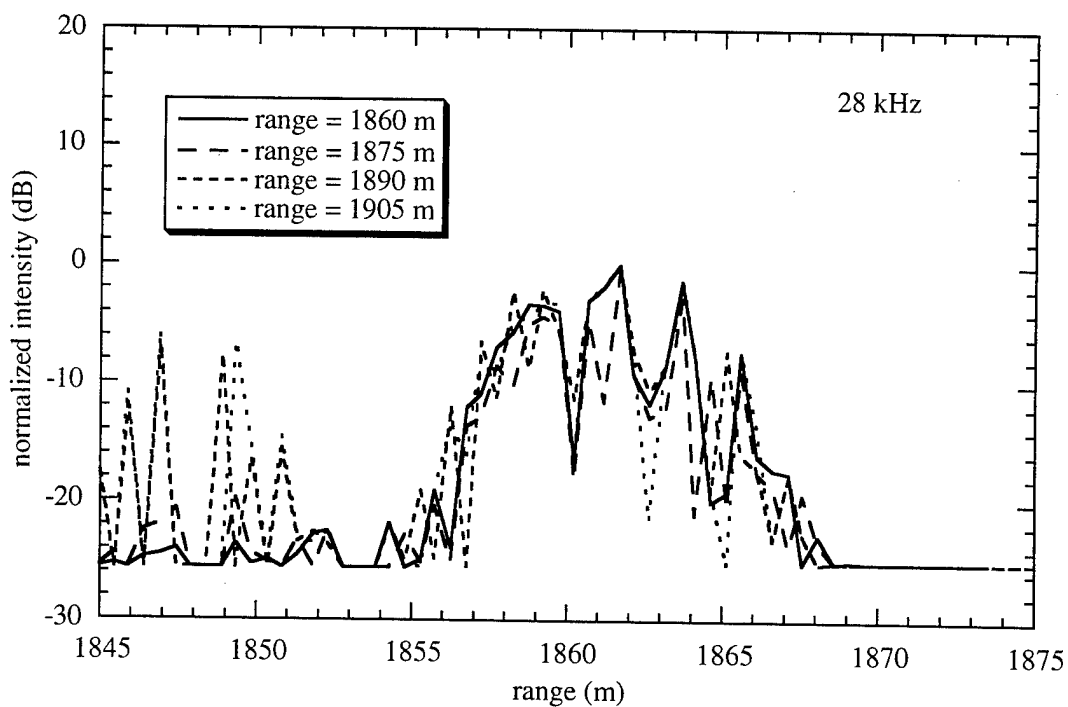


Figure 18: GSM results at 28 kHz for ranges of 1860 m, 1875 m, 1890 m, 1905 m. The four curves were time shifted to align the maximum of each curve.

prior to averaging. This meant that each ping had an equal weighting and ensured that no single ping dominated the average, thereby providing a more effective comparison with GSM.¹² In the subsequent discussion, we shall refer to the data normalized to zero dB at its maximum *prior* to averaging as the weighted data, and the data normalized to zero dB at its maximum *after* averaging as the unweighted data. Note that the data shown previously in Figures 11, 14, and 17 were unweighted.

A. GSM/Data Time Spreading Comparisons at 21 kHz

Figure 19 contains a comparison of the average of the modelled echoes for the 21 kHz sequence with both the weighted and unweighted average for the 21 kHz data, for a nominal SEAHORSE to echo repeater separation of 1400 m. Squares represent the weighted-average data, open circles represent the unweighted-average data, and the solid line represents the model estimate. The GSM eigenray output (not shown) indicates that the direct path is neither the dominant arrival nor the earliest arrival. It is rather labourious (and not particularly instructive) to associate each modelled peak with its respective eigenray due to the combined effect of the two-way propagation employed in the model and the averaging of the model output. However, it is worth mentioning by way of example that the dominant eigenray for the 21 kHz data is the ray that departs SEAHORSE upward (i.e. toward the surface), then refracts downward and finally refracts upward before arriving at the echo repeater. This eigenray is the emboldened solid line in Figure 7. For comparison, the first arrival is the single bottom reflection path shown as the emboldened dashed line in Figure 7.

Clearly, there is less than perfect agreement between the model and the experimental data. The model does however, explain the dominant feature in the data – the asymmetry of the data about its peak amplitude. This feature is consistent with the distribution of peaks predicted by GSM. That is to say, GSM predicts far fewer arrivals prior to the dominant peak than after. Although secondary peaks are not visible in the data, the relative amplitudes of the peaks in the model are consistent with the general decay in amplitude of the data after the arrival of the dominant peak. Furthermore, recalling Figure 7, the dominant peak in Figure 19 has no surface or bottom interaction whereas the peak at 1395 m as well as peaks located at 1405 m and beyond have bottom and/or surface interactions. This provides phenomenological evidence at least that one might alter the bottom reflection coefficients in Table II to reduce these secondary peaks without reducing the dominant one, thereby improving the fit between GSM and the data. However, without quantitative information on the bottom parameters, the exercise would not be particularly instructive. More importantly, any improvement in the fit is unlikely to account for the discrepancy between the data and the model in the immediate vicinity of the dominant peak. That is to say, there is significant time spreading of the dominant data peak beyond that attributable to multipath propagation. It seems unlikely that the spreading in the data results from ocean surface motion since the model predicts no surface interaction for the dominant path. Nor is platform motion likely to be responsible since both SEAHORSE and the echo repeater were nearly motionless.

B. GSM/Data Time Spreading Comparisons at 28 kHz

Figure 20 contains a comparison of the average of the modelled echoes at 28 kHz with both the weighted and unweighted average for the 28 kHz data. The nominal separation from SEAHORSE to the echo repeater during this ping sequence was 1860 m. Squares represent the weighted average of the data, open circles represent the unweighted average of the data, and a solid line represents the model estimate. As in the 21 kHz case, the structure of the data is reasonably well modelled by GSM. The small undulations in

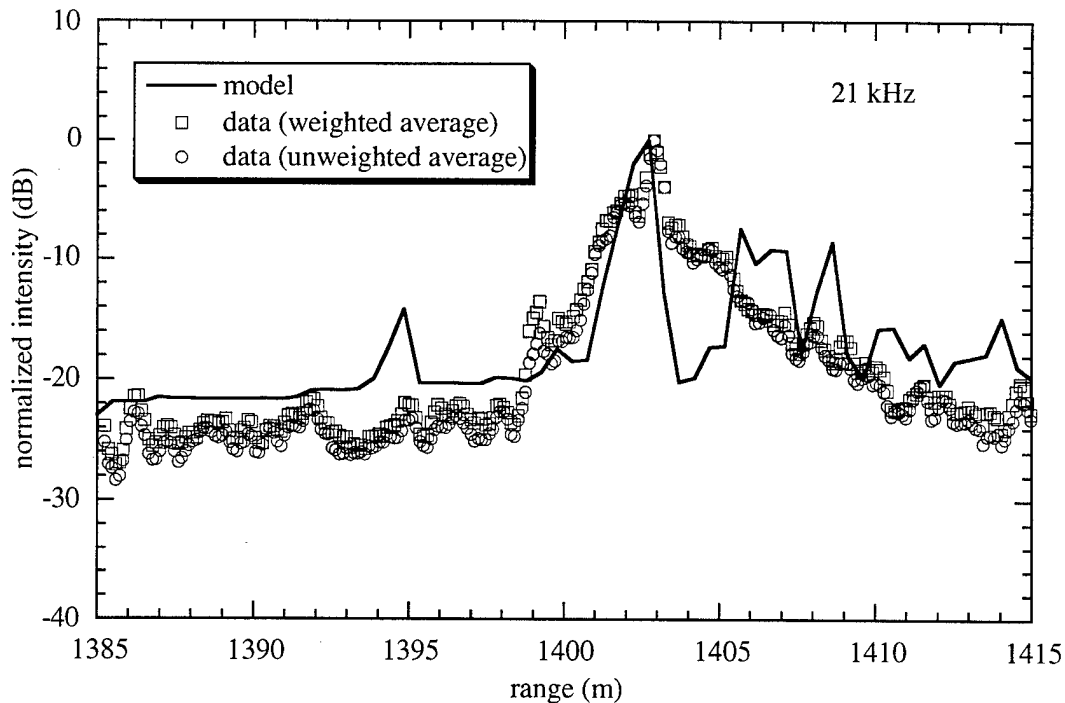


Figure 19: Averaged time spreading data for the 16 pings at 21 kHz, compared to the averaged output of the Generic Sonar Model for 16 ranges at 2 m increments (solid line). Both a weighted data average (squares), computed by normalizing to 0 dB prior to averaging, and an unweighted data average (circles), computed by normalizing after averaging are shown. (Refer to text.)

the data from 1845 m to 1853 m may correspond to the three small peaks in the model at 1846, 1849, and 1852 m. Both data and model are significantly more symmetric about the maximum than at 21 kHz. The 28 kHz data are time spread relative to the ideal matched filter (recall Figure 14). However, the model results suggests that multipath propagation should have resulted in even greater time spreading than that exhibited by the data. However, this discrepancy between GSM and the data may result from inaccuracies in the bottom loss and backscattering strength tables as discussed previously.

C. GSM/Data Time Spreading Comparisons at 36 kHz

Figure 21 contains a comparison of the average of the modelled echoes at 36 kHz with both the weighted and unweighted data, for a nominal SEAHORSE to echo repeater separation of 1950 m. Squares represent the weighted average of the data, open circles represent the unweighted average of the data, and a solid line represents the model estimate. Once again the structure of the data is reasonably well modelled by GSM. The peaks in the model that occur from 1935 m to 1940 m roughly correspond to peaks in the evenly weighted data. Note that none of these peaks are clearly visible in the unweighted data. As with the 28 kHz case, the model predicts more extensive time spreading about the main peak than is exhibited by the data.

V. DISCUSSION

The energy calculation of the standard deviation indicates that there is significant ping-to-ping variability in the energy. This likely occurs as ping-to-ping fluctuations redistribute the energy into paths which don't intercept the target, or as more energy is

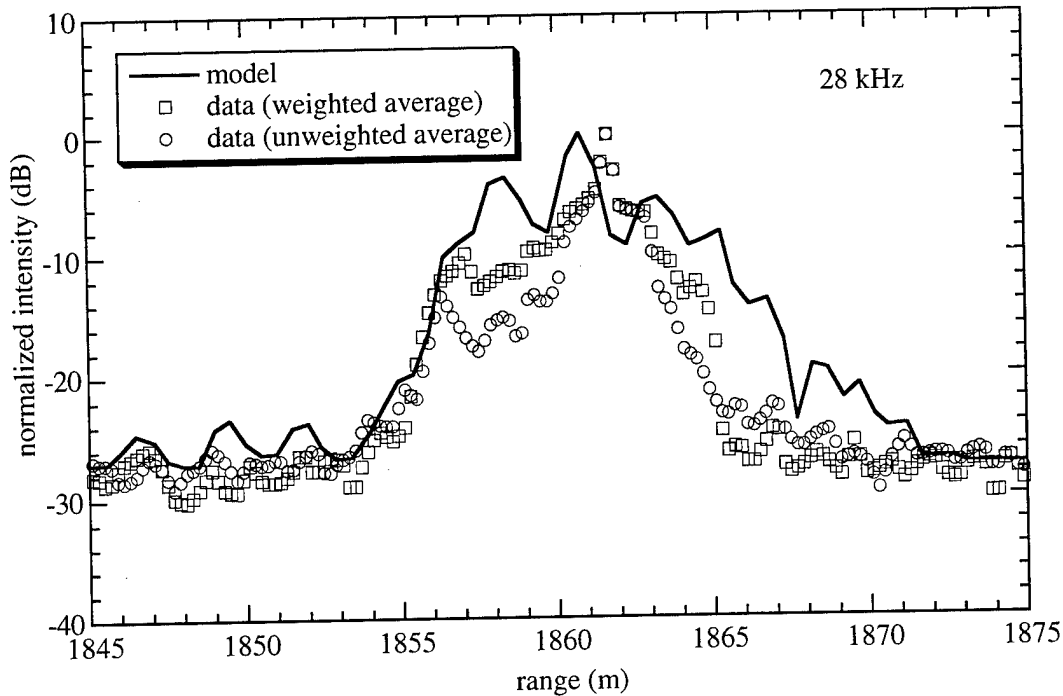


Figure 20: Averaged time spreading data for the 16 pings at 28 kHz, compared to the averaged output of the Generic Sonar Model for 16 ranges at 2 m increments (solid line). Both a weighted data average (squares), computed by normalizing to 0 dB prior to averaging, and an unweighted data average (circles), computed by normalizing after averaging are shown. (Refer to text.)

scattered incoherently through surface and/or bottom interactions from one ping than from another. No attempt was made to model this because GSM lacks a realistic fading model for individual eigenrays. That is to say, the GSM results do not have any statistical fluctuations built into the eigenray calculation – partly because GSM is not a range-dependent model.

At all three frequencies, the standard deviation was lower when computed using the total energy than when computed using the peak value. (Recall Table I.) This is because the peak value calculation results from a single eigenray and small changes in range affect the amount of energy in the dominant eigenray. In contrast, the energy calculation is less sensitive to these fluctuations since a significant portion of the energy stripped from one eigenray will reach the receiver via a slightly different path(s). Note that the *difference* in the value of the standard deviation obtained from the energy calculation and the peak level calculation is in good agreement with the standard deviation of 1 dB obtained from the model, which was cited in the previous section.

Although GSM provides a qualitative explanation of the time spreading, there are definite discrepancies between the model and the data. For example, the 21 kHz data in Figure 19 exhibits significantly more time spreading immediately after the arrival of the dominant peak than estimated by the model. Also, in Figures 20 and 21, the several well defined peaks around the maximum obtained from GSM are not all observable in the data. It is reasonable to assume that the agreement would improve if one had more accurate inputs into GSM for the bottom loss, the backscattering strength, and the SEAHORSE-to-target separation for each ping. However, the range-independent nature of GSM will clearly limit one's ability to match the fine structure of the data.

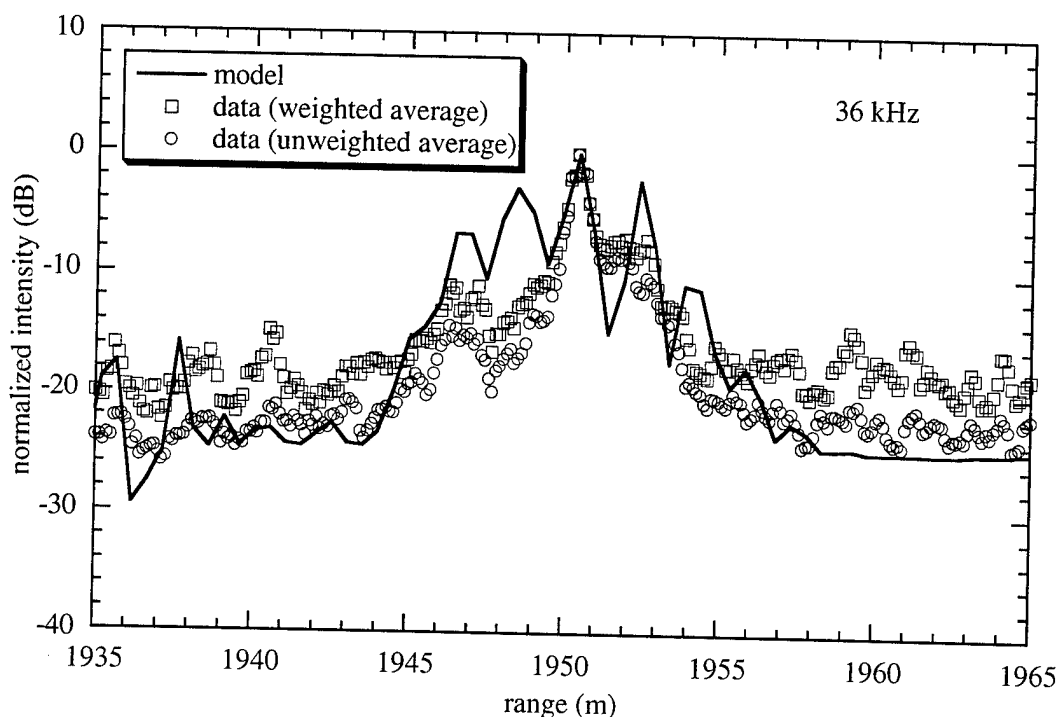


Figure 21: Averaged time spreading data for the 16 pings at 36 kHz, compared to the averaged output of the Generic Sonar Model for 16 ranges at 5 m increments (solid line). Both a weighted data average (squares), computed by normalizing to 0 dB prior to averaging, and an unweighted data average (circles), computed by normalizing after averaging are shown. (Refer to text.)

VI. SUMMARY AND CONCLUSIONS

Time spreading measurements were collected in water 100 m deep, off the coast of Nova Scotia. Data were collected at center frequencies of 21 kHz, 28 kHz, and 36 kHz using linear FM pulses 0.16 s in duration with a 2-kHz bandwidth. Canada's SEAHORSE array, an anchored, high frequency active sonar was employed for the source-receiver, and a UK free-drifting echo repeater was employed for the target. Source-receiver and target position were recorded using a portable target range operated by the US. At each frequency, time-spreading measurements obtained from averaging the returns from 16 pings were compared with estimates obtained from the Generic Sonar Model (GSM). Additionally, the standard deviation of the received echo intensity from the 16 pings was computed.

The standard deviation of the received echo intensity was computed two ways. First it was computed from the peak echo level from each of the 16 pulses at a given frequency. Then, it was computed from the total energy received from each of the 16 pings. At all three frequencies, the standard deviation was lower by 1 to 2 dB when computed from the total received energy. This is likely because the maximum value results from a single eigenray and the energy in the dominant eigenray closely depends on small changes in range, etc. In contrast, the energy calculation is less sensitive to these fluctuations since a significant portion of the energy will still reach the receiver via slightly different paths.

At each frequency, the average time spreading was computed and normalized to 0 dB with respect to the maximum. These data were compared to the output of an ideal matched filter with the following results. At 21 and 28 kHz, little or no time spreading occurred in the region of the peak, down to about the -4 dB points. Below -4 dB however, the time spreading increases substantially. At 36 kHz, the time spreading only becomes significant below the -8 dB points.

GSM provides an acceptable qualitative explanation of the time spreading, particularly in describing the overall width and shape of the main returns. At 21 kHz, the time spreading data were extremely asymmetric about the maximum in the data whereas at 28 and 36 kHz the data were somewhat more symmetric. The GSM results indicate that the degree of symmetry resulted from the arrival time and amplitude of the various eigenrays. There were some definite discrepancies between the model and the data. At 21 kHz, the data exhibited significantly more time spreading in the vicinity of the maximum than estimated by the model. At 28, and 36 kHz the GSM output exhibited several clear peaks which were not well defined in the data. It is reasonable to expect the agreement to improve if one had more accurate inputs into GSM for the bottom loss, the backscattering strength, and the SEAHORSE-to-target separation for each ping. However, the range-independent nature of GSM will clearly limit one's ability to match the fine structure of the data.

ACKNOWLEDGMENTS

The authors wish to acknowledge the contributions of the experimental teams. The ARL-PSU and ARL-Keyport teams of John Fleck, Ron Hoy, John Keller, Mike Roeckel, Steve Moss, Brian Rotsten, and Dan Shades were led by Dr. R. Lee Culver. The NUWC-Keyport team of Jerry Armstrong, Ralph Evenson, and Dave Romanko was led by Mr. Dan Jepsen. The DRA Portland team of Deryk Bryant and Alex Vincent was led by Dr. Martin Bishop. The DREA team included Dr. Roger Chan, Mark O'Connor, Grant Stocker, Mark Radcliffe, Roger Arsenault, George Gill, and Bob MacDonald. The authors also wish to acknowledge NUWC for release of GSM to DREA and Mr. James Theriault of DREA for his assistance in preparing the GSM results.

REFERENCES

- ¹ H. Weinberg, "The Generic Sonar Model," Naval Underwater Systems Center, New London, CT, Technical Document 5971D, 1985.
- ² Paul C. Hines, J. Stuart Hutton, and Arthur J. Collier, "A Free Floating, Steerable, HF Sonar for Environmental Measurements," IEEE Oceans '93 Conference Proceedings, Vol. 2, pp. 65-70, 1993.
- ³ R. Lee Culver, Applied Research Laboratory, The Pennsylvania State University, in preparation.
- ⁴ Throughout the paper, when multiple time spreading data sets are plotted in a single figure the curves are shifted to align the peak returns. It should be noted that the maximum time shift required to align the peaks for a given frequency equated to a range change of ± 25 meters about the mean separation of SEAHORSE and the echo repeater. That is to say, the separation was approximately constant for any frequency run.

-
- ⁵ Clearly, none of the 16 returns will correspond exactly to the mean level. The curve referred to as the mean target return is actually the curve *nearest in level* to the mean value calculated from the 16 pulses analyzed.
- ⁶ Note that we computed the standard deviation on the logarithmic (decibel) value of the peaks.
- ⁷ For the purposes of computation, we approximate the total energy of a curve to include the area under the curve down to -20 dB below its peak level.
- ⁸ Using a Tukey-shaded transmit pulse and 50% overlap in the fast convolution routine ensures that the smearing loss is less than 1 dB.
- ⁹ Paul C. Hines and Dale D. Ellis, "*High-Frequency Reverberation in Shallow Water*", J. Oceanic Engineering, Special Issue on Shallow Water Acoustics, Geophysics, and Oceanography, July 1997.
- ¹⁰ Since the time of writing, side scan sonar data have been obtained at the site. Once analyzed, these data will provide a more quantitative description of the bottom.
- ¹¹ The modelled source level at the echo repeater was obtained by *incoherently* summing the arrivals on the various eigenrays. The modelled received level at SEAHORSE was obtained by *incoherently* summing the arrivals on the eigenrays.
- ¹² A consequence of the small standard deviation in the model (≈ 1 dB) is that the weighted and unweighted averages obtained from the model are very similar. In the data-model comparison that follows, the authors have used the unweighted averages obtained from the model.

UNCLASSIFIED

SECURITY CLASSIFICATION OF FORM
(highest classification of Title, Abstract, Keywords)

DOCUMENT CONTROL DATA <small>(Security classification of title, body of abstract and indexing annotation must be entered when the overall document is classified)</small>		
1. ORIGINATOR (The name and address of the organization preparing the document. Organizations for whom the document was prepared, e.g. Establishment sponsoring a contractor's report, or tasking agency, are entered in section 8.) Defence Research Establishment Atlantic P.O. Box 1012, Dartmouth, N.S. B2Y 3Z7	2. SECURITY CLASSIFICATION <small>(Overall security of the document including special warning terms if applicable.)</small> <p style="text-align: center; font-size: 1.2em;">Unclassified</p>	
3. TITLE (The complete document title as indicated on the title page. Its classification should be indicated by the appropriate abbreviation (S,C,R or U) in parentheses after the title.) <p style="text-align: center; font-size: 1.2em;">Time Spreading at High Frequency in a Shallow Water Channel</p>		
4. AUTHORS (Last name, first name, middle initial. If military, show rank, e.g. Doe, Maj. John E.) <p style="text-align: center;">HINES, Paul C., COLLIER, Arthur J. and HUTTON J. Stuart</p>		
5. DATE OF PUBLICATION (Month and year of publication of document.) <p style="text-align: center; font-size: 1.2em;">September 1996</p>	6a. NO. OF PAGES (Total containing information. Include Annexes, Appendices, etc.) <p style="text-align: center; font-size: 1.2em;">27</p>	6b. NO. OF REFS. (Total cited in document.) <p style="text-align: center; font-size: 1.2em;">12</p>
6. DESCRIPTIVE NOTES (The category of the document, e.g. technical report, technical note or memorandum. If appropriate, enter the type of report, e.g. interim, progress, summary, annual or final. Give the inclusive dates when a specific reporting period is covered.) <p style="text-align: center; font-size: 1.2em;">Technical Memorandum</p>		
8. SPONSORING ACTIVITY (The name of the department project office or laboratory sponsoring the research and development. include the address.) Defence Research Establishment Atlantic P.O. Box 1012, Dartmouth, N.S. B2Y 3Z7		
9a. PROJECT OR GRANT NUMBER (If appropriate, the applicable research and development project or grant number under which the document was written. Please specify whether project or grant.) <p style="text-align: center;">1.c.2</p>	9b. CONTRACT NUMBER (If appropriate, the applicable number under which the document was written.) 	
10a. ORIGINATOR'S DOCUMENT NUMBER (The official document number by which the document is identified by the originating activity. This number must be unique to this document.) <p style="text-align: center; font-size: 1.2em;">DREA Technical Memorandum 96/209</p>	10b. OTHER DOCUMENT NUMBERS (Any other numbers which may be assigned this document either by the originator or by the sponsor.) 	
11. DOCUMENT AVAILABILITY (Any limitations on further dissemination of the document, other than those imposed by security classification) <div style="margin-left: 20px;"> <input checked="" type="checkbox"/> Unlimited distribution <input type="checkbox"/> Distribution limited to defence departments and defence contractors; further distribution only as approved <input type="checkbox"/> Distribution limited to defence departments and Canadian defence contractors; further distribution only as approved <input type="checkbox"/> Distribution limited to government departments and agencies; further distribution only as approved <input type="checkbox"/> Distribution limited to defence departments; further distribution only as approved <input type="checkbox"/> Other (please specify): </div>		
12. DOCUMENT ANNOUNCEMENT (Any limitation to the bibliographic announcement of this document. This will normally correspond to the Document Availability (11). However, where further distribution (beyond the audience specified in 11) is possible, a wider announcement audience may be selected.) 		

UNCLASSIFIED

SECURITY CLASSIFICATION OF FORM

DDO3 2/06/87

UNCLASSIFIED
SECURITY CLASSIFICATION OF FORM

13. **ABSTRACT** (a brief and factual summary of the document. It may also appear elsewhere in the body of the document itself. It is highly desirable that the abstract of classified documents be unclassified. Each paragraph of the abstract shall begin with an indication of the security classification of the information in the paragraph (unless the document itself is unclassified) represented as (S), (C), (R), or (U). It is not necessary to include here abstracts in both official languages unless the text is bilingual).

Time spreading measurements provide an indirect measure of the acoustic bandwidth that can be supported by the water channel, which is critical to the design of sonar systems. Time spreading measurements were collected in a water channel 100 m deep, off the coast of Nova Scotia. Data were collected at frequencies of 20-22 kHz, 27-29 kHz, and 35-37 kHz using linear FM pulses 2 s in duration. The experiments were part of a collaborative TTCP trial known as Trial Scotian (HF) organized by the Environmental Acoustic specialists group of GTP-11, Underwater Weapons and Countermeasures. Canada, the US, and the UK participated in the trial. Canada's SEAHORSE array, an anchored, high frequency active sonar was employed for the source-receiver, and a UK free drifting echo repeater was employed for the target. Source-receiver and target position were recorded using a portable tracking range operated by the US. In the paper, time spreading measurements are compared with modelled estimates obtained using the Generic Sonar Model (GSM). The GSM estimates of time spreading due to multipath propagation compare favourably with the experimental data. However, time spreading of individual paths – beyond the model predictions – is also evident. Additionally, the data were used to compute the standard deviation of the received echo intensity at each frequency. The standard deviation was computed two different ways. First it was computed using the peak echo level from each of the pulses at a given frequency. Then, it was computed from the total energy received from each of the pings. At all three frequencies, the standard deviation was lower by 1 to 2 dB when computed from the total received energy.

14. **KEYWORDS, DESCRIPTORS or IDENTIFIERS** (technically meaningful terms or short phrases that characterize a document and could be helpful in cataloguing the document. They should be selected so that no security classification is required. Identifiers, such as equipment model designation, trade name, military project code name, geographic location may also be included. If possible keywords should be selected from a published thesaurus. e.g. Thesaurus of Engineering and Scientific Terms (TEST) and that thesaurus-identified. If it not possible to select indexing terms which are Unclassified, the classification of each should be indicated as with the title).

**TIME SPREADING
UNDERWATER ACOUSTICS
SHALLOW WATER
LINEAR FM**

UNCLASSIFIED
SECURITY CLASSIFICATION OF FORM